ASSESSING LOCATION CAPABILITY WITH GROUND TRUTH EVENTS: THE DEAD SEA AND SOUTH AFRICA REGIONS

Clifford Thurber, Haijiang Zhang, and William Lutter

University of Wisconsin-Madison

Sponsored by Defense Threat Reduction Agency

Contract No. DSWA01-98-1-0008

ABSTRACT

We are combining locally derived ground truth (GT) information with analyses of regionally recorded waveform data to derive path corrections to global network stations for earthquakes and explosions in the Dead Sea and South Africa regions. Our strategy is to determine locations that are quality GT5 or better for events using "local" information, and then to treat these locations as known, fixed hypocenters in a regional joint hypocenter determination (JHD) inversion for the path corrections. We are using arrival time picks from all available waveform data from global network stations in the inversion for path corrections.

For the Dead Sea region, we are using data from 53 earthquakes and the 3 Dead Sea calibration explosions to derive local 1-D velocity models and station corrections for about 70 seismic network stations within Israel and Jordan, using JHD. The explosions are treated as sources with known (fixed) location and origin time in the JHD inversion. The resulting locations for the earthquakes are constrained quite well, with estimated 95% confidence regions ranging from 1 to 3 km in both epicenter and depth. Thus, we feel confident in treating these earthquakes as GT5 events. The next step is to use a smaller group of events with data available at regional and teleseismic distances as "master events" with fixed locations in a regional JHD solution for path corrections to global network stations. We also investigate the use of "surrogate" stations to interpolate path corrections at IMS stations without observations. For South Africa, we have obtained ground-truth information on mining-induced earthquakes from the seismology investigators (T. Jordan and D. James) who operated the PASSCAL South African craton broadband experiment. We identified 14 events having regional and teleseismic waveforms that could be used for location calibration purposes, and we were provided with locations (including depths) determined from mine records for these events. As in the case of the Dead Sea investigation, the next step is to use the larger events in our Dead Sea dataset as "master events" with fixed locations in a regional JHD solution for path corrections to global network stations. We present our results for the Dead Sea and South Africa path corrections along with an assessment of the location accuracy that can be obtained via their use. We also examine the ability to estimate IMS station path corrections using path corrections from nearby non-IMS stations. A nearest-neighbor interpolation algorithm performs well at predicting the IMS station path corrections in most cases.

KEY WORDS: location, ground truth, corrections, calibration

OBJECTIVE

We are combining locally derived ground truth (GT) information with analyses of regionally recorded waveform data to derive path corrections to International Monitoring System (IMS) and global network stations for earthquakes and explosions in the Dead Sea and South Africa regions. Our location calibration strategy is to determine locations that are quality GT5 or better for events using "local" information, and then to treat these locations as known, fixed hypocenters in a regional joint hypocenter determination (JHD) inversion for the path corrections. We are using arrival time picks from all available waveform data from global network stations in the inversion for path corrections. We then use the path corrections at non-IMS stations to estimate corrections for nearby IMS stations with no available observations and use the GT event data to assess location accuracy.

RESEARCH ACCOMPLISHED

Dead Sea region

In November 1999, three underwater chemical explosions were conducted in the Dead Sea (Gitterman and Shapira, 2001). According to the authors, the goals of that experiment were "to calibrate the regional travel times and propagation paths of seismic waves across the Middle East and the Eastern Mediterranean region and thus improve location accuracy of seismic events; to calibrate local, regional, and International Monitoring System (IMS) stations; and to provide data for source characterization to improve IMS detection, location, and discrimination capabilities." With the GT information of these three calibration explosions, we have relocated 53 regional earthquakes through JHD analysis using arrival time picks at stations in Israel and Jordan. The P-wave arrival times were determined by us from the original digital waveform data (50 events) or were obtained from the Prototype International Data Centre (pIDC) (3 events).

We performed JHD analysis using the algorithm VELEST (Kissling et al., 1994). VELEST produced a best-fitting layered velocity model, station corrections for 73 seismic network stations within Israel and Jordan, relocated event locations and origin times, and estimated uncertainties of the event locations and origin times. The GT information for these 57 events is provided in Table 1, and the event locations are plotted in Figure 1, along with the local stations.

From the above 53 earthquakes, 10 with available regional data were used in a regional JHD inversion, combined with one calibration explosion (991111) and another earthquake (991028) without ground truth information. These events are indicated with an asterisk in Table 1. Event 991028 was added based on its available arrival time data at many IMS stations. The locations and origin times for the other 11 events were restrained to those from the VELEST GT results in the JHD solution. We used velocity model ak135 in our JHD analysis. We obtained path corrections for many regional stations, including 17 IMS stations, which are presented in Table 2. The number of observations of these events using just IMS stations is too small to allow for a thorough location error analysis.

One important issue is whether or not path corrections for new IMS stations can be estimated from nearby ("surrogate") stations with a longer history of observations. We used non-IMS stations in the region less than 5° away from IMS stations to find the relationship between their path corrections. For example, IMS station HFS has four neighboring non-IMS stations (see Table 3). We interpolated an estimated HFS station correction from its neighboring stations with a two-dimensional "nearest neighbor" (NN) interpolation method. The interpolated path correction using NN is -2.09 s, in excellent agreement with the value in Table 2 (-2.17 s). We also interpolated other IMS path corrections using neighboring stations and various interpolation methods, and compared the results with the known station corrections. From the comparison, we found that the two-dimensional NN interpolation method produced superior results. Using this approach, we can interpolate path corrections at other IMS stations using their neighboring stations. The results are shown in Table 4. We note, however, that variations in station elevations may have a significant effect on this interpolation approach. This problem will receive further investigation.

South Africa region

For the South Africa region, we obtained GT data on events of magnitude 3.5 to 4.5 from T. Jordan and D. James, who had carried out a broadband seismic array study across the region in 1997-1999. These events are mining-induced earthquakes. They obtained event locations from mine operators, who run local seismic networks at the mines but do not use a standard time base, and origin times from the Geological Survey of South Africa or the ISC. The GT locations for the 14 events used are presented in Table 5.

P-wave arrival times were picked from original digital waveform data obtained from the Center for Monitoring Research and from the IRIS Data Management System. Waveform data were obtained for a number of stations in Africa (Figure 2), for stations up to 45° epicentral distance. In parallel, we obtained pIDC picks for the same 14 events to provide a greater sampling of stations. As in the case of the Dead Sea events above, the arrival times of both datasets (digital and pIDC) were used in JHD solutions for path corrections, keeping all events fixed at their GT locations, but fixing just the master event's origin time

(980821). The resulting path corrections are given in Table 6, consolidated from the two solutions, and the origin times from the digital JHD solution are given in Table 5.

We selected the same event, the one with the largest number of observations (980821; 7 observations), to use as the master event for a test of relocation accuracy to simulate a Comprehensive Nuclear-Test-Ban Treaty (CTBT) monitoring scenario, using just the digital dataset. The other 13 events had between 3 and 6 observations. The JHD results were quite good, with 9 events having mislocations of less than 7 km, and the other 4 events having mislocations ranging from 12 to 16 km (Figure 3), despite the small number of observations and poor azimuthal coverage. Thus, all of the events would meet the 1000 km^2 location accuracy criterion of the CTBT (National Research Council, 1997). We note that the larger event mislocations are all shifted towards the east, consistent with an elongation of the confidence ellipses in the east-west direction. Our next step will be to examine the improvement in locations that can be obtained when waveform cross-correlation is used to determine the arrival times.

CONCLUSIONS AND RECOMMENDATIONS

We have utilized "local" GT information in two very different cases, the Dead Sea and South Africa regions, to explore our ability to derive path corrections that can be used to derive relatively accurate event locations. In the Dead Sea case, a "local" JHD analysis was used to derive the GT information, whereas in the South Africa region, we were able to obtain GT location information from a local source. We carried out JHD analyses for both datasets to determine path corrections to IMS and other stations.

We used the Dead Sea results to test interpolation methods for estimating path corrections for IMS stations from those at nearby non-IMS stations. The NN method proved to be effective. We anticipate that kriging would also be effective. One issue requiring further investigation is the effect of varying station elevations on this path correction estimation approach. We used the South Africa results to provide another test of location accuracy using sparse regional-distance data. We found that event locations could be determined to the level of accuracy desired for CTBT monitoring. We also are confident that the accuracy can be improved substantially with the application of waveform cross-correlation for this dataset.

ACKNOWLEDGEMENTS

We acknowledge the assistance of Nitzan Rabinowitz, Xiaoping Yang, and the IRIS Data Management System in obtaining the waveform data used in this study. We are also extremely grateful to Tom Jordan and David James for sharing their information on event locations in South Africa.

REFERENCES

Gitterman, Y. and A. Shapira (2001), Dead Sea Seismic Calibration Experiment Contributes to CTBT Monitoring, *Seism. Res. Lett.*, 72, 159-170.

Kissling, E., W.L. Ellsworth, D. Eberhart-Phillips, and U. Kradolfer (1994), Initial Reference Models in Local Earthquake Tomography, *J. Geophys. Res.*, 99, 19,635-19,646.

National Research Council (1997), Research Required to Support Comprehensive Nuclear-Test-Ban Treaty Monitoring, National Academy Press, Washington, D.C.

Table 1. Ground Truth data for earthquakes in the Dead Sea region: origin time, latitude, longitude, depth (in km), and uncertainties; * denotes events used in the regional analysis.

#	YRMODA	HRMN	SEC	LAT	LON	DEP	?OT	?X	? Y	? Z
1	000327	1505	48.03	31.7296	35.5660	22.2	0.3	1.4	1.5	0.7
2	000328	0103	18.65	31.7325	35.5437	22.7	0.3	1.4	1.5	0.9
3	000412	0047	47.89	31.2774	35.5558	10.0	0.3	1.3	1.3	0.9
4	000705	0333	51.48	31.4870	35.5844	12.8	0.3	1.4	0.9	1.0
5	880303	2339	26.73	31.4737	35.5572	7.1	0.4	0.6	1.3	0.4

6	890218	0019	55.28	31.6869	35.5135	13.0	0.4	0.2	1.1	0.4
7	891218	1133	40.92	31.4490	35.6203	1.6	0.3	0.4	0.8	0.3
8	900326	1352	12.02	31.4678	35.5560	7.1	0.4	0.6	1.1	0.3
9	910623	1302	22.24	31.2920	35.4887	0.9	0.1	1.1	1.1	0.4
10	910623	2222	57.53	31.2924	35.4742	-0.2	0.1	1.2	1.0	0.4
11	910624	2047	10.86	31.5646	35.4959	16.7	0.3	0.8	1.5	0.9
12	910905	0817	5.81	31.7110	35.4344	-0.1	0.1	0.6	1.6	0.4
13	910905	2102	0.60	31.2836	35.4988	1.1	0.3	1.2	1.0	0.4
14	910927	2224	54.13	31.0700	35.4527	1.0	0.3	0.9	0.7	0.3
15	910930	1155	41.56	31.0750	35.4488	0.6	0.1	0.8	0.5	0.4
16	911004	0817	25.12	31.0703	35.4644	1.1	0.3	0.8	0.6	0.3
17	911128	1311	51.06	31.2000	35.3631	-0.4	0.1	1.0	1.3	0.4
18	920102	1837	42.79	31.4325	35.5493	0.6	0.1	0.6	1.5	0.4
19*	920111	0346	31.52	31.2409	35.3843	5.9	0.4	0.9	1.2	0.3
20	920626	1641	35.17	31.0915	35.4129	8.9	0.4	0.3	0.3	0.8
21*	920626	1717	45.23	31.0810	35.4271	9.2	0.4	0.7	0.4	0.8
22	920907	0257	52.74	31.3068	35.4698	1.5	0.3	1.1	1.3	0.4
23	921008	0517	51.62	31.2943	35.4085	10.4	0.3	1.0	0.9	1.2
24	921128	0149	09.20	31.4025	35.4298	7.5	0.4	0.9	1.4	0.4
25	930528	0322	46.61	31.0879	35.4364	0.9	0.1	0.9	0.7	0.4
26	930704	2305	51.42	31.8905	35.4417	0.0	0.1	1.0	1.5	0.4
27*	930802	0912	56.71	31.5025	35.4957	23.5	0.3	0.6	1.4	0.9
28*	930802	2316	53.03	31.3138	35.4089	23.5	0.3	0.9	1.0	1.0
29	931104	2112	29.13	31.4191	35.5424	3.4	0.3	0.4	1.4	0.2
30	931125	0710	33.30	31.8229	35.6046	0.2	0.1	1.0	1.6	0.4
31	950327	2349	46.34	31.5291	35.4990	0.5	0.1	0.7	1.5	0.4
32	950825	0525	05.63	31.3685	35.4785	1.3	0.3	0.8	1.1	0.4
33	950825	0548	52.18	31.4237	35.4113	0.6	0.1	1.0	1.5	0.5
34	951118	1842	28.04	31.4225	35.5512	10.3	0.4	0.7	1.2	0.4
35	960414	1330	34.83	31.3933	35.3437	0.9	0.1	1.5	1.5	0.4
36	960830	0920	42.75	31.3892	35.3977	22.3	0.3	1.4	1.4	1.1
37*	961010	1136	35.36	31.5194	35.4192	0.3	0.1	1.4	1.4	0.3
38	970904	0820	06.48	31.4190	35.4289	1.0	0.2	0.6	1.1	0.5
39	970923	1523	54.70	31.4615	35.4591	10.2	0.3	0.9	1.5	0.5
40	970926	0706	28.77	31.4719	35.4653	5.2	0.4	0.8	1.0	0.1
41	971002	0045	37.58	31.4569	35.4628	11.7	0.4	0.8	1.2	0.4
42*	940916	0318	56.88	32.0599	35.5273	18.8	0.2	1.3	1.3	1.4
43*	840824	0602	23.95	32.7265	35.1350	-0.4	0.1	1.6	1.6	0.3
44	870427	2041	46.71	31.2222	35.5421	8.0	0.3	1.1	1.5	1.0
45	880226	1751	05.31	31.6740	35.5377	20.8	0.3	0.5	1.6	1.2
46	890118	0100	50.96	32.5128	35.4544	3.5	0.2	1.6	1.3	1.5
47	890412	2111	48.37	31.6631	35.5252	16.5	0.2	1.4	1.4	1.6
48	890426	2128	55.45	31.3195	35.4775	4.1	0.3	1.0	1.4	0.2
49	890701	1404	34.21	31.7814	35.5687	4.5	0.2	1.5	1.5	0.2
50	901010	0040	58.52	31.4915	35.5216	6.1	0.2	0.7	1.6	0.5
51*	920729	0530	47.06	32.4029	35.4592	9.1	0.2	1.4	1.2	1.2
52*	920910	1953	43.64	31.9075	35.1281	15.1	0.2	1.5	1.3	1.4
53*	951128	2110	52.59	29.7573	34.9987	3.4	0.3	1.5	1.2	1.3
54*	991028	1539	13.66	30.4500	35.0749	-	-	-	-	-
55	991108	1300	00.33	31.5330	35.4460	0.0	0.0	0.0	0.0	0.0
56	991110	1359	58.20	31.5340	35.4460	0.0	0.0	0.0	0.0	0.0
57*	991111	1500	00.78	31.5350	35.4460	0.0	0.0	0.0	0.0	0.0

Table 2. IMS station path corrections from the Dead Sea regional JHD analysis. Corrections are in seconds.

STA	LAT	LON	CORR
ARCE	69.535	25.506	-4.41
ARU	56.430	58.562	-1.46
BGCA	5.176	18.424	0.50
CMAR	18.458	98.943	-5.98
DAVO	46.839	9.794	-0.01
EKA	55.333	-3.159	-1.79
ESDC	39.676	-3.962	-0.66
FINE	61.444	26.077	-3.57
FRB	63.747	-68.547	5.92
HFS	60.134	13.697	-2.17
INK	68.307	-133.520	3.44
MBC	76.242	-119.360	-1.26
MLR	45.492	25.944	1.05
OBN	55.167	36.600	-2.56
PDY	59.633	112.700	-3.70
SPIT	78.178	16.370	-4.21
YKA	62.493	-114.605	6.47

Table 3. Comparison of Dead Sea path corrections at nearby stations - IMS station HFS example.

STA	LAT	LON	CORR
HFS	60.134	13.697	-2.17
SLL	60.476	13.320	-2.18
KONO	59.649	9.598	-1.76
UPP	59.858	17.627	-1.98
APP	60.539	13.928	-2.05

Table 4. Interpolated path corrections at IMS stations for Dead Sea region events.

STA	LAT	LON	CORR
ABKT	37.9304	58.1189	0.2
BJT	40.0183	116.1679	7.4
BORG	64.7474	-21.3268	3.2
BRAR	39.8535	32.7608	0.3
DBIC	6.6701	-4.8563	-2.2
ILAR	64.7714	146.8866	-1.7
JHJ	33.1200	139.8200	5.3
KBZ	43.7286	42.8975	2.8
KVAR	43.9557	42.6952	2.7
MJAR	36.5247	138.2070	5.3
NOA	61.0397	11.2148	-2.0
NORES	60.7353	11.5414	-1.1
NRIS	69.0061	87.9964	-0.6
PARD	32.9308	35.4343	0.0
SADO	44.7694	-79.1417	8.1
SCHQ	54.8319	-66.8336	-2.5
ULM	50.2486	-95.8755	5.9
VRAC	49.3083	16.5935	-1.3
ZAL	53.9367	84.7981	-1.2

Table 5. Ground Truth data for South Africa events: origin time, latitude, longitude, depth (km).

YRMODA	HR	MIN	SEC	LAT	LON	Depth
970729	11	25	5.35	-27.9577	26.7022	0.68
970801	02	17	26.93	-27.9492	26.6992	-0.03
970925	00	05	23.04	-26.3709	27.5166	-1.26
971212	16	42	46.46	-26.9664	26.7481	-0.63
980821	16	10	53.30	-26.9536	26.7705	-1.24
980925	15	51	31.31	-26.9259	26.8057	-0.59
981002	10	17	53.34	-26.3953	27.4703	-0.48
981117	20	17	59.34	-26.9319	26.7880	-0.88
981118	16	30	5.43	-26.9461	26.7812	-1.19
981205	04	52	44.31	-26.3597	27.6112	-3.11
990107	15	18	55.28	-26.9185	26.7299	-1.30
990202	10	33	21.79	-26.4356	27.4130	-0.81
990226	09	27	47.49	-26.3876	27.4278	-0.39
990422	22	19	37.34	-27.9338	26.7128	0.33

Table 6. Path corrections for IMS and other stations based on the South Africa regional JHD analysis. Corrections (CORR) and estimates uncertainties (ERR) are in seconds.

STA	LAT	LON	CORR	#OBS	ERR
ARU	56.430	58.562	0.38	1	0.67
BDFB	-15.644	-48.014	0.43	6	0.33
BGCA	5.176	18.424	-1.56	11	0.06
BOSA	-28.614	25.256	0.26	14	0.06
BRAR	39.853	32.761	1.58	5	0.35
CMAR	18.457	98.943	0.15	9	0.32
CPUP	-23.331	-57.329	-6.97	3	0.42
DAVO	46.839	9.794	-4.15	1	0.67
DBIC	6.670	-4.856	-0.74	5	0.07
EIL	29.670	34.951	-0.21	1	0.67
ESDC	39.675	-3.962	0.38	14	0.25
FINE	61.444	26.077	0.66	11	0.26
GERE	48.845	13.702	1.15	9	0.29
KBZ	43.729	42.898	1.09	1	0.67
LBTB	-25.015	25.597	1.09	12	0.06
LPAZ	-16.288	-68.131	0.74	7	0.33
LSZ	-15.277	28.188	-2.00	3	0.08
MAW	-67.604	62.871	1.32	6	0.31
MSKU	-1.656	13.612	-1.66	1	0.13
NOA	61.040	11.215	1.37	3	0.39
NORE	60.735	11.541	1.56	4	0.38
PLCA	-40.731	-70.550	0.06	1	0.67
RAYN	23.522	45.503	-0.46	1	0.13
SUR	-32.380	20.812	0.07	12	0.06
TSUM	-19.202	17.584	-1.78	8	0.06
VNDA	-77.514	161.846	1.15	5	0.35

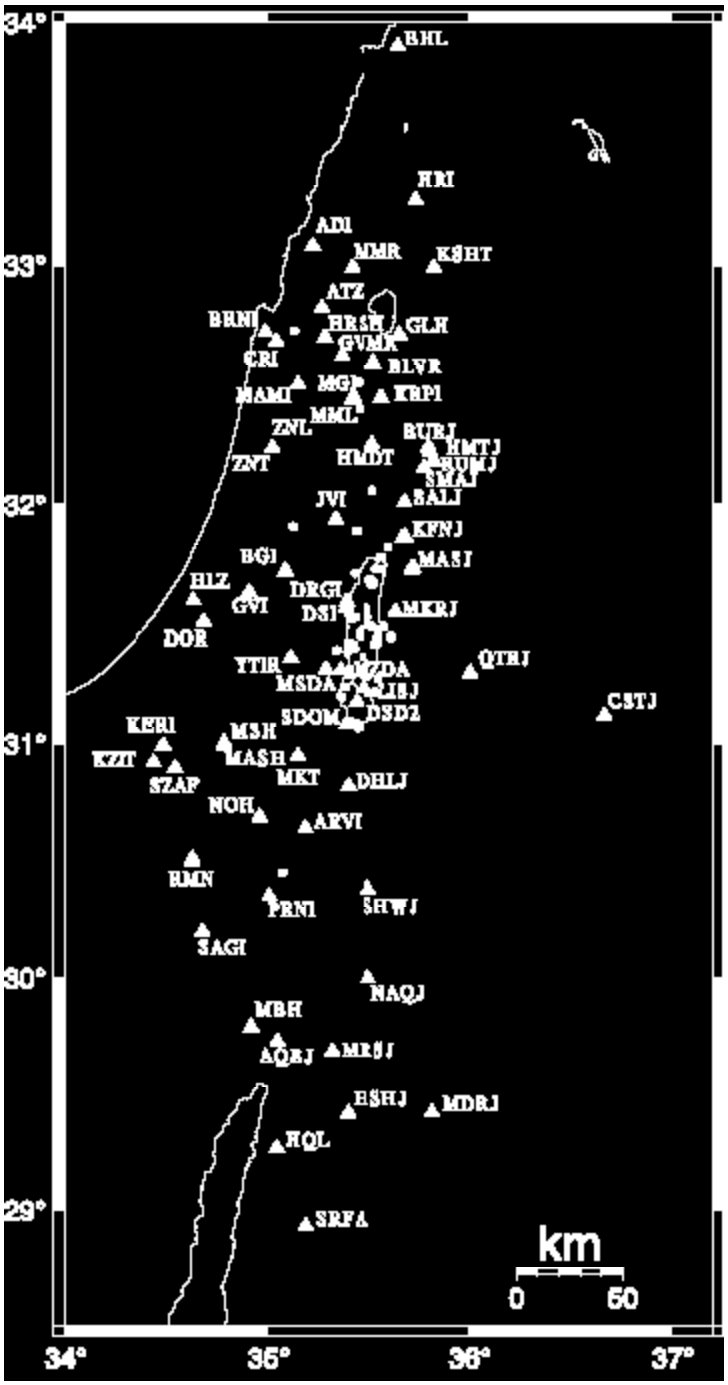

Figure 1. Stations (triangles) and events (circles) used in JHD analysis to derive GT locations for determining path corrections for IMS and other regional stations.

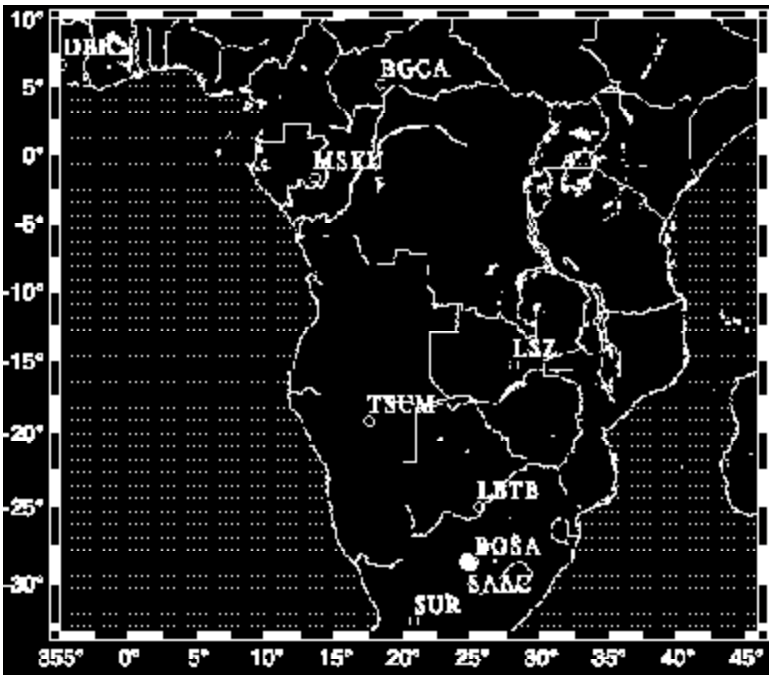

Figure 2. Stations in Africa for which digital waveform data were obtained for events listed in Table 5.

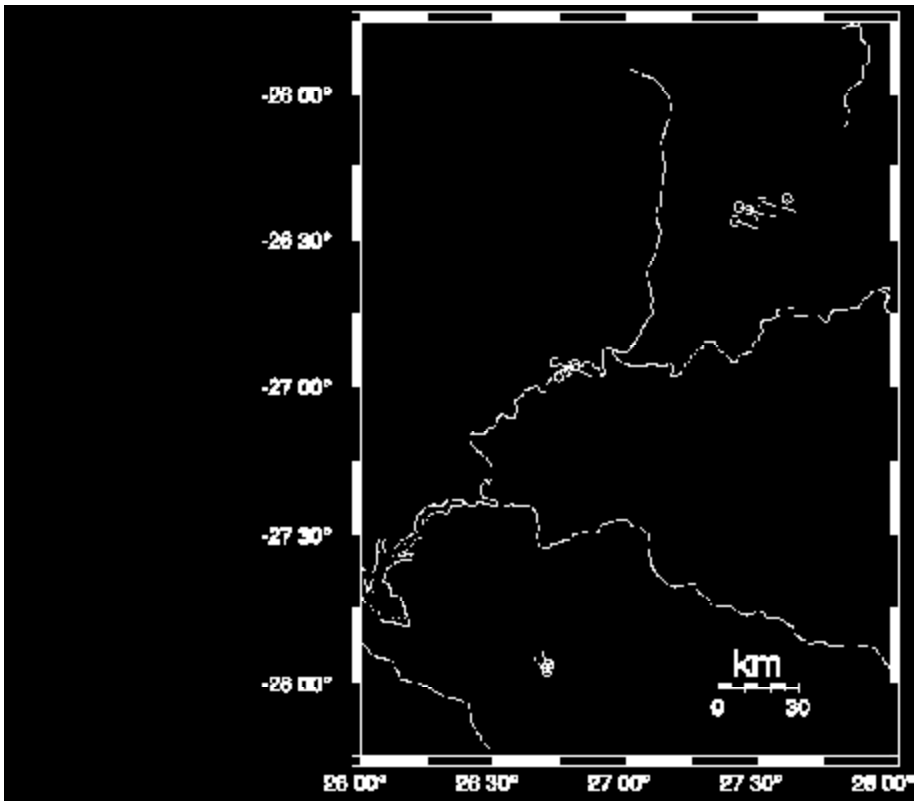

Figure 3. Event mislocations (tails on circles) using one master event (980821) in a JHD solution.